

Dry-Cooled Rankine Cycle Operated with Binary Carbon Dioxide Based Working Fluids

Viktoria Illyés¹[\[https://orcid.org/0000-0002-4030-6958\]](https://orcid.org/0000-0002-4030-6958), Salma Salah²[\[https://orcid.org/0000-0001-7541-1320\]](https://orcid.org/0000-0001-7541-1320),
Abdelrahman Abdeldayem²[\[https://orcid.org/0000-0003-0114-405X\]](https://orcid.org/0000-0003-0114-405X), Andreas Werner¹[\[https://orcid.org/0000-0002-7107-802X\]](https://orcid.org/0000-0002-7107-802X), Abdalnaser Sayma²[\[https://orcid.org/0000-0003-2315-0004\]](https://orcid.org/0000-0003-2315-0004), Giampaolo Manzolini³[\[https://orcid.org/0000-0001-6271-6942\]](https://orcid.org/0000-0001-6271-6942), and Markus Haider¹[\[https://orcid.org/0000-0002-0054-4206\]](https://orcid.org/0000-0002-0054-4206)

¹ TU Wien, Austria

² City University of London, UK

³ Politecnico di Milano, Italy

Abstract. The dry-cooled Rankine cycle working with a zeotropic mixture of CO₂+C₆F₆ is influenced by the ambient temperature as air is used as the heat sink. Varying heat sink temperatures allow for operating the cycle under sliding condensation pressure which may benefit a hybrid PV-CSP plant. The study demonstrates the effect of this operation mode on composition shift and condensation pressure and investigates the cycle performance. The results show that defining the turbine design conditions significantly impact whether the system's thermodynamic performance behaves acceptably in off-design conditions. Operating the turbine which was designed for a big pressure ratio in part-load especially if both, inlet and outlet pressure are at off-design conditions, is not favorable and leads to deteriorated efficiencies. Under some constraints for turbine and heat exchanger design, the proposed cycle enhances the hybrid PV-CSP system.

Keywords: Rankine Cycle, Transcritical Cycle, CO₂-Based Mixtures

1. Introduction

1.1 Hybrid PV-CSP

The disadvantages of using solar energy are as apparent as the advantages: Annual and daily variability of solar energy limits the (annual) capacity factor to a great extent. Hybrid PV-CSP systems are an interesting way of improving the capacity factor as well as providing base load coverage by a stable power output, [1]. In this work, the proposed system is a non-compact PV-CSP hybrid system with a Solar Tower (ST) and thermal energy storage (TES) as shown in Figure 1. Still, the CSP plant and the TES need further research and development to convince in terms of cost and reliability, [2]. Particle systems may soon prove to be the choice of technology for TES especially when coupled with solar particle receivers, [3].

This current study analyzes the power cycle of the SCARABEUS-concept and whether it benefits the hybrid system. The focus is on the influence of ambient temperature on the working fluid's composition and its conditions on the low pressure side of the system as dry-cooling is one of the main advantages of the proposed cycle.

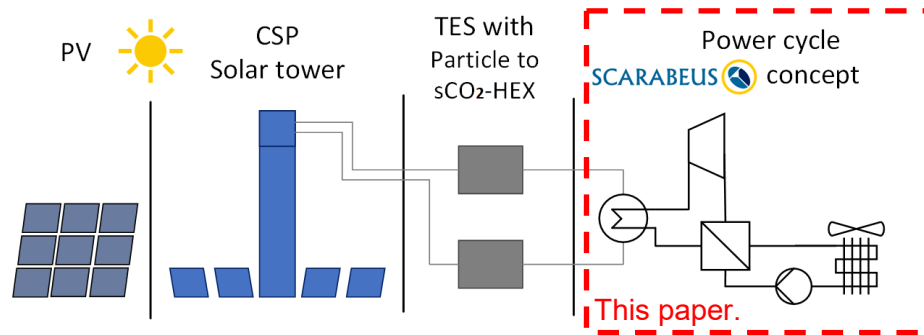


Figure 1. Concept and focus of this paper.

1.2 The SCARABEUS-concept

A promising concept for boosting conversion efficiency and reducing the cost of the CSP plant are power blocks working with supercritical carbon dioxide (sCO₂) as a working fluid. Very high temperatures are feasible with sCO₂, which improves the cycle efficiency. Moreover, the working fluid's high density throughout the process allows for compact turbomachinery components and lower costs than a conventional steam Rankine cycle. Nevertheless, at high minimum temperatures, the supercritical CO₂ cycle shows significant compression work. An interesting solution to overcome this hurdle are CO₂-based working fluids that enable the transcritical Rankine cycle.

When CO₂ and an additive with a high critical temperature are combined into a binary mixture, the critical temperature increases with respect to pure CO₂ while keeping the advantages of sCO₂ cycles when compared to steam Rankine cycles. Mixtures with high critical temperature allow for condensation at higher temperatures than possible for pure CO₂. Then, on the one hand, dry cooling with ambient air becomes feasible and water usage is drastically reduced or even set to zero. Secondly, a pump is adequate to operate in the liquid subcritical region, where the working fluid's compressibility is minor. The simpler layout and liquid compression are clear advantages of this concept.

Besides costs, it has been shown that cycles with CO₂-based mixtures present higher thermomechanical efficiencies than the reference CO₂ cycle. Crespi et al. [4] analyzed the promising candidates hexafluorobenzene C₆F₆, titaniumtetrachloride TiCl₄ and sulfur dioxide SO₂. The optimized working fluids each present higher thermal efficiencies for a turbine inlet temperature of 550°C and a high pressure of 250bar than the reference pure CO₂ cycle in at least one of the cycle layouts: Recuperated Rankine, Recompression or Precompression. The gain in efficiency can be seen in Figure 2. Pure CO₂ shows the best performance when operated in a Recompression cycle, leading to thermal efficiencies of 42.7%. With a C₆F₆ molar fraction of 15%, the Precompression cycle shows a thermal efficiency of 43.6%.

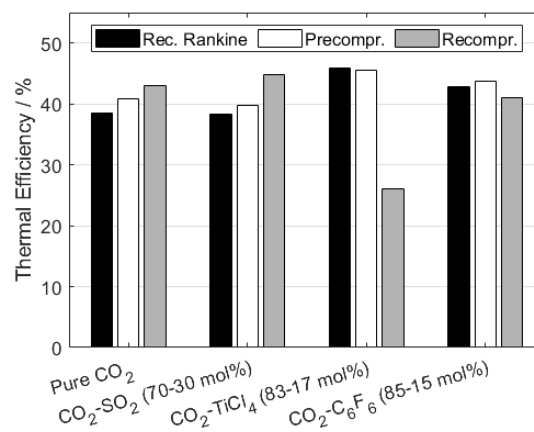


Figure 2. Cycle efficiencies of pure CO₂ and mixture cycles for three layouts, data from [3].

The use of CO₂-based mixtures as working fluids is studied and detailed within the SCARABEUS project, an EU H2020 project, with the target of reducing the levelized cost of electricity of CSP plants by using these innovative working fluids.

2. Cycles with zeotropic mixtures: composition shift and sliding condensation pressure method

Zeotropic mixtures are used in refrigeration systems, heat pumps and power cycles because of their thermodynamic performance and a temperature glide at the heat input and heat rejection. For solar application, Organic Rankine Cycles (ORC) and Kalina cycles are operated and studied [5]. These mixtures are not within the target range of the SCARABEUS-concept in terms of the many constraints: high thermal stability, high critical temperature, being environmentally and operationally safe, cheap and available. Hexafluorobenzene (C₆F₆) has been identified as one promising candidate as it has a critical temperature of 244°C, moderate flammability and is stable up to about 600°C, when a nickel-based alloy is used for tubing, [6]. Under these conditions, a 100h static thermal stability test was performed.

The low pressure side of the Rankine cycle is determined by the temperature of the heat sink. Thermodynamic cycles with zeotropic mixtures experience composition shifts if cooling temperature varies, as the vapor liquid equilibrium (VLE) is determined by temperature, pressure and composition of the mixture. E.g., it has been found that a composition shift influences the ORC performance significantly, [7].

The conventional way is to design the dry-cooled power cycle with a fixed working point at the VLE determined by the local maximum ambient temperature. If there are lower cooling temperatures available, which would result in lower condensation pressures, higher efficiencies can be expected. A study on Kalina cycles showed that this sliding condensation pressure method improves the annual average efficiency even more than a composition tuning method [8].

2.1 Methods and Modelling

This work on the simple recuperative cycle working with the CO₂+C₆F₆ mixture is developed in four major steps as graphically shown in Figure 3: 1. determination of the vapor liquid equilibrium, 2. design and recalculation of the turbine, 3. calculating the thermodynamic cycle, and 4. design and recalculation of the condenser. The four methodology steps are detailed in the following subsections. The properties for the mixture are obtained with the Peng-Robinson method and a binary interaction parameter of $k_{ij}=0.033$ according to [9].

Two main off-design condition sets for the turbine and the simple recuperated Rankine cycle are analyzed as reported in Table 1: the sliding condensation pressure method in full load, which means changing the condensation/turbine outlet pressure, and part-load conditions, meaning accepting a lower turbine inlet pressure to reduce mass flow. The influence of two turbine designs on the cycle is computed, A and B for highest and lowest pressure ratio (PR).

Table 1. Off-design calculations for two turbine designs A and B.

Off-design	Turbine design A	Turbine design B
	for highest PR	for lowest PR
sliding condensation pressure	~30°C T _{cond}	~20°C T _{cond}
sliding condensation pressure	~40°C T _{cond}	~30°C T _{cond}
sliding condensation pressure	~50°C T _{cond}	~40°C T _{cond}
sliding condensation pressure	~54°C T _{cond}	~50°C T _{cond}

part-load (~54°C T_{cond})	~45% m°_{design}	~45% m°_{design}
part-load (~54°C T_{cond})	~60% m°_{design}	~60% m°_{design}
part-load (~54°C T_{cond})	~70% m°_{design}	~70% m°_{design}
part-load (~54°C T_{cond})	~85% m°_{design}	~85% m°_{design}

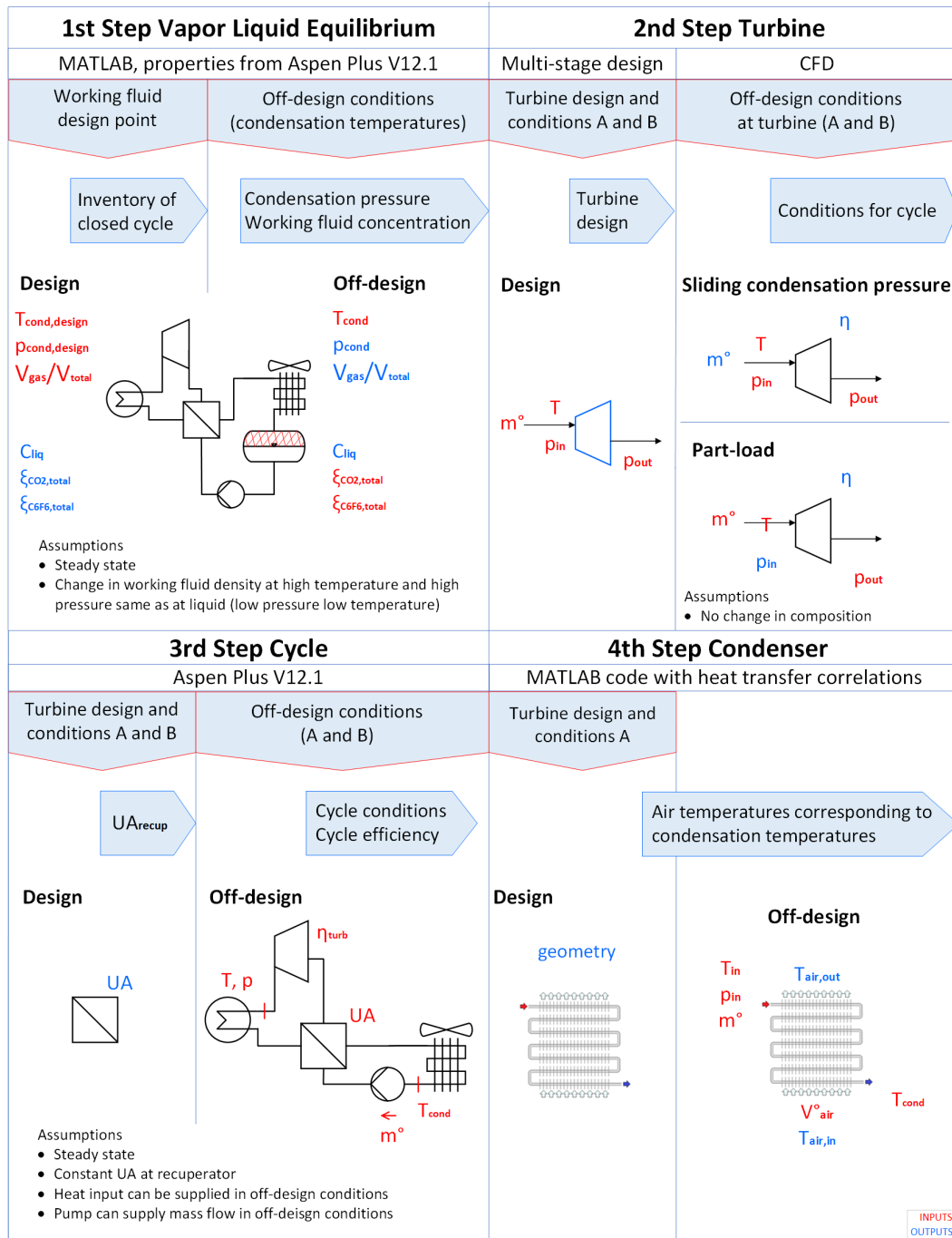


Figure 3. Calculation steps, their methods, in- and outputs.

2.2 Cycle calculation (step 3)

The proposed layout is a recuperated Rankine cycle, see Figure 4. Inputs to the cycle are summarized in Table 2 for turbine design A exemplarily.

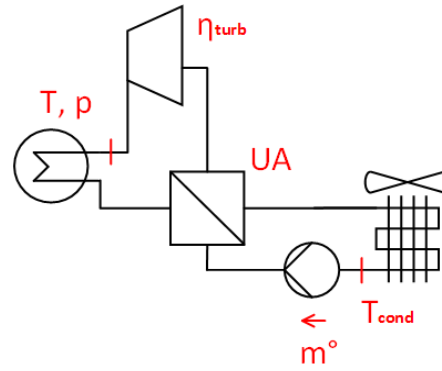


Figure 4. Cycle layout and input to cycle calculations.

Cycle calculations are executed in Aspen Plus V12.1. For the recuperator, a design temperature approach of 5K is used to size the component and in off-design, a constant heat transmission coefficient (constant UA) is assumed. In reality, the heat transmission coefficient U will decrease in part load. This will decrease the “overdesign-effect” in part load. The other heat exchangers, heater and condenser, are only modeled for working fluid side. Calculated inlet- and outlet conditions of the condenser will link the ambient air temperature to the cycle after Aspen simulations are done in the 4th step. The heat input is assumed variable not only in part-load but also in sliding condensation pressure method to supply a turbine inlet temperature (TIT) of 550°C in all cases. The primary heat exchanger and TES would need to be designed accordingly. Correlating ambient temperature with heat input or season is not part of this analysis. The pump is assumed to supply the cycle’s high pressure at any conditions. The total-to-static efficiency from CFD is used as an estimation of the isentropic efficiency. After the condenser, an isobaric subcooling of 2K was assumed.

Table 2. Inputs to cycle with indications of inputs (with asterix) and outputs (without asterix) of previous calculations for case A; for design (D), sliding condensation pressure (SCP), part-load (PL).

	1. VLE	1. VLE	1. VLE	2. Turb.	2. Turb.	2. Turb.	2. Turb.	2. Turb.
	T_{cond}	p_{cond}	x_{CO_2}	TIT	$P_{turb,in}$	PR	m°	η_{turb}
	°C	bar	mol. frac.	°C	bar	/	kg/s	%
D	20.02*	46.92	86.73%*	550*	253*	5.12*	1218.0*	93.15
SCP	30.00*	56.61	86.69%	550*	253*	4.28*	1215.6	90.12
SCP	40.01*	67.89	86.71%	550*	253*	3.59*	1205.9	88.30
SCP	49.75*	79.50	86.87%	550*	253*	3.09*	1193.7	85.74
SCP	53.86*	84.50	87.00%	550*	253*	2.91*	1185.9	84.29
PL	53.86*	84.50	87.00%	550*	134.6	1.54	548.1*	44.39
PL	53.86*	84.50	87.00%	550*	166.02	1.90	730.8*	68.07
PL	53.86*	84.50	87.00%	550*	199.97	2.28	913.5*	77.93
PL	53.86*	84.50	87.00%	550*	223.35	2.55	1035.3*	81.56

Table 3. Further in- and outputs, fixed for all cycle calculations.

Δp_{heater}	4	bar	$\Delta p_{recup,cold}$	0.5	bar
Δp_{cond}	1.5	bar	$\Delta T_{pinch,recup,design}$	5	K
$\Delta p_{recup,hot}$	0.5	bar	$\Delta T_{subcool}$	2	K

2.3 Vapor liquid equilibrium (step 1): C₆F₆ design point and off-design

In the first step, the working fluid's circulating composition is determined: The design point for choosing the composition is a trade-off between condensation temperature (preferably high), condensation pressure (preferably low), a significant margin to the critical point (preferably high) and amount of additive in the mixture (preferably low). This combination was chosen for the circulating C₆F₆-mixture, see Figure 5:

- Condensation temperature of 54°C
- Condensation pressure of 84.5bar
- Molar fraction of CO₂ 87 % and C₆F₆ 13%
- Critical point at 92°C and 120bar

As shown in Figure 3, the liquid working fluid arrives in the tank where it is in equilibrium with the gas phase of a different composition if steady state conditions are assumed. Knowing the condensation temperature, pressure and composition of the liquid phase, the composition of the gas phase is concluded. The system needs to be filled with the mixture in charging composition. The correlation of circulating and charging composition is visualized in Pxy-diagrams, see Figure 6. The curves are valid for a constant temperature of 54°C and a constant pressure of 84.5bars, respectively. In the Pxy-diagram, the conditions of the circulating (liquid) flow, the gas volume in the tank and the total charging mixture lie on the line of constant pressure at 84.5bar. The total/charging composition is in the two-phase-region and is determined by the amount of gas phase in the system in design case, which was set to $V_{\text{gas}}/V_{\text{total}}=5\%$.

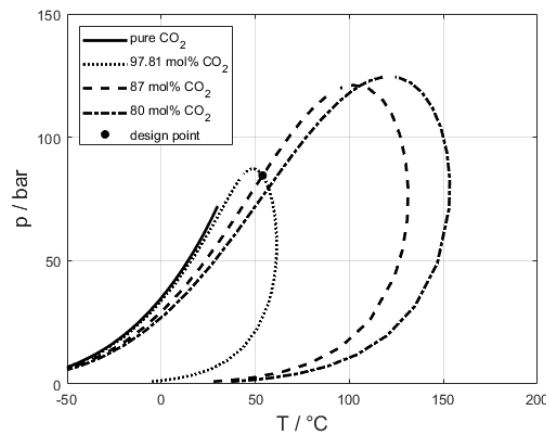


Figure 5. PT-diagram for pure CO₂ and C₆F₆-CO₂ mixtures.

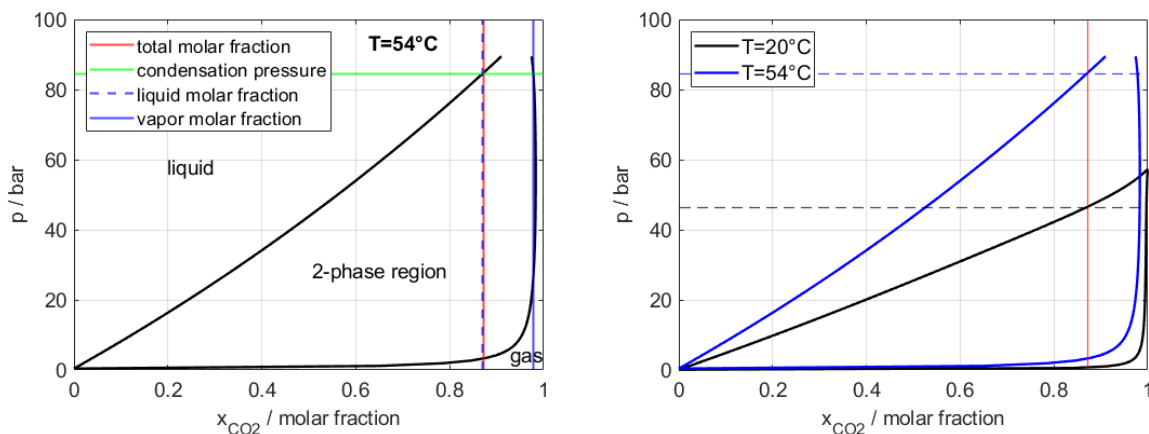


Figure 6. Pxy-diagram, left: VLE at 54°C, right: comparison of two temperatures.

The fixed inventory of charging composition is in a closed system; thus, changing the state in this system is an isochoric process. The condensation pressure and composition of the liquid phase result from the assumption of a perfect equilibrium at a certain temperature. The change of volume due to thermal expansion of the liquid phase in the components at different conditions is neglected as these components are not sized. This means that the density change in the circulating flow is the same as in the liquid at equilibrium. This is a fair assumption for the sliding condensation pressure conditions, in which cases the system's high pressure (and high temperature) is always kept at the same value. For part-load conditions, this assumption might lead to significant deviations.

2.4 Turbine (step 2): design and off-design

Secondly, the turbine is designed for two design conditions: A) the highest possible pressure ratio (PR) and B) the lowest possible pressure ratio, corresponding to the lowest and highest possible condensation temperature. The performance of the turbine in off-design conditions is calculated in CFD. For the sliding condensation pressure method, the turbine back pressure is varied; therefore, the pressure ratio is varied accordingly. The mass flow rate and efficiency are output values. The turbine inlet pressure is changed for the part load cases to achieve a certain reduced mass flow rate.

In the current study, the two turbine designs were developed at the operating conditions as reported in Table 1 and Table 2 in red and a rotational speed of 3000rpm:

- A 12-stage turbine design was developed at a pressure ratio of 5.24 which is referred to as design A.
- A 14-stage turbine, design B, was developed for the lowest pressure ratio of 2.89.

The turbine designs were developed based on previously set aerodynamic, rotor-dynamic and mechanical design criteria where the static bending stress and slenderness ratio, the ratio of the total axial flow path length with respect to the hub diameter, of 130MPa and 9.0 were specified [10]. To predict the aerodynamic turbine performance, the multi-stage design tool was integrated with the Aungier loss model [11] where profile, secondary flow, trailing edge and tip clearance loss are considered. Furthermore, the 3D blades design was generated using the obtained mean-line design parameters with 3D geometrical parameters adjusted to satisfy the required mass flow-rate for the given pressure boundary conditions. It is worth mentioning that a mesh independence study was carried out to determine the optimum mesh size considering the solution accuracy alongside with the computational effort. The generated 3D blade model was evaluated at different operating and boundary conditions to assess the model performance at part-load and in sliding condensation pressure operation.

The corrected mass flow and efficiency trends differ when changing the pressure ratio by changing the turbine's inlet and outlet pressure as shown in Figure 7. Increasing the outlet pressure to smaller PR results in a significant drop in efficiency, while the mass flow does not drop accordingly fast. When changing the inlet pressure, the high efficiency can be maintained for higher PR, and, until a certain point also for smaller PR where a rapid drop occurs. Part-load conditions are reasonable by changing the inlet pressure only.

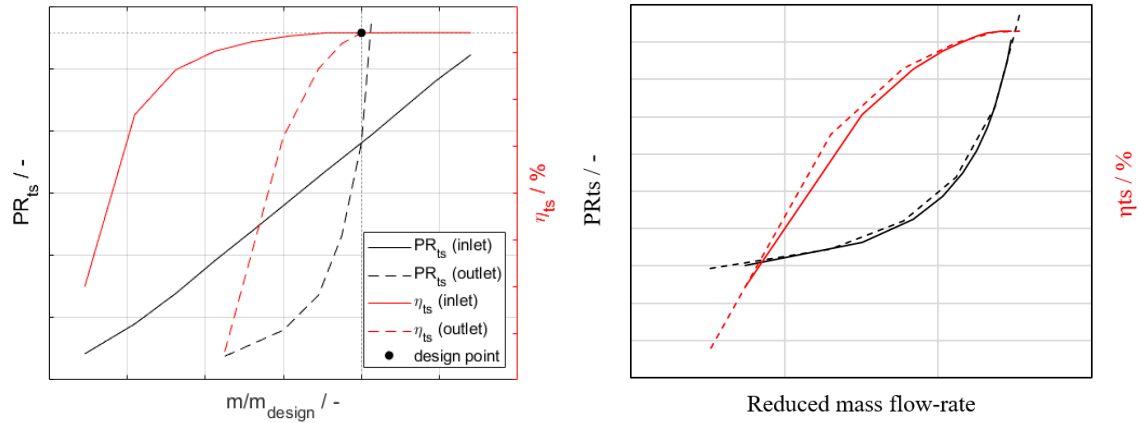


Figure 7. Pressure ratio and efficiency trends at off-design when the inlet or outlet pressure is varied, obtained for an axial turbine operating with C₆F₆/CO₂ mixture, left: against the mass flow-rate ratio to the design mass flow-rate, right: against the non-dimensional reduced mass flowrate.

2.5 Condenser (step 4): Air-cooled condenser calculation

In the last step, the link between the ambient air temperature and cycle conditions is evidenced. After determining the size and geometry of the air-cooled condenser (ACC), the air inlet temperature is found with which a certain condensation temperature can be achieved.

By this calculation, the condensation temperature in the cycle gets linked to ambient air temperature. Moreover, the effects of operating the condenser in off-design conditions can be analyzed. The ACC model and its validation is described in detail in [12]. The cross-flow heat exchanger has horizontal tubes with circular fins on the outside. The model uses the following heat transfer correlations: Cavallini [13] and the Bell and Ghaly [14] correction term on the working fluid side and the Grimison model for staggered tubes at the air side. The pressure drop inside the tubes is computed by the Del Col et al. [15] model. The effectiveness of each cell determines the heat balance, according to Navarro and Cabezas-Gómez [16].

The ACC is designed for the design case A conditions and an air inlet and outlet temperature of 5 and 22°C, an air face velocity of 3m/s and a mixture pressure drop of 1.5 bar.

3. Results and Discussion

3.1 Trends of condensation pressure and circulating composition

The results from the VLE calculations are shown in Figure 8. The change of condensation pressure when varying the total composition in the system is not significant for relevant inputs, namely between 0-10% gas volume in the design case. The line for 100% gas volume shows the upper boundary of the calculation and does not have practical relevance. The condensation pressure may also be approximated by the bubble pressure of the design concentration without major consequences. All lines meet in the design point. The lines end at different higher temperatures, which indicates the end of the two-phase region, so the working fluid would be at supercritical state at temperatures above those shown.

The change in composition is also minor: For the lowest condensation temperature of the cycle analysis, 20°C, the difference in composition for 0 and 10% gas volume in design is only 0.27 percentage points of molar fraction. A significant change in composition only occurs at significant design gas volumes, which are not of practical relevance.

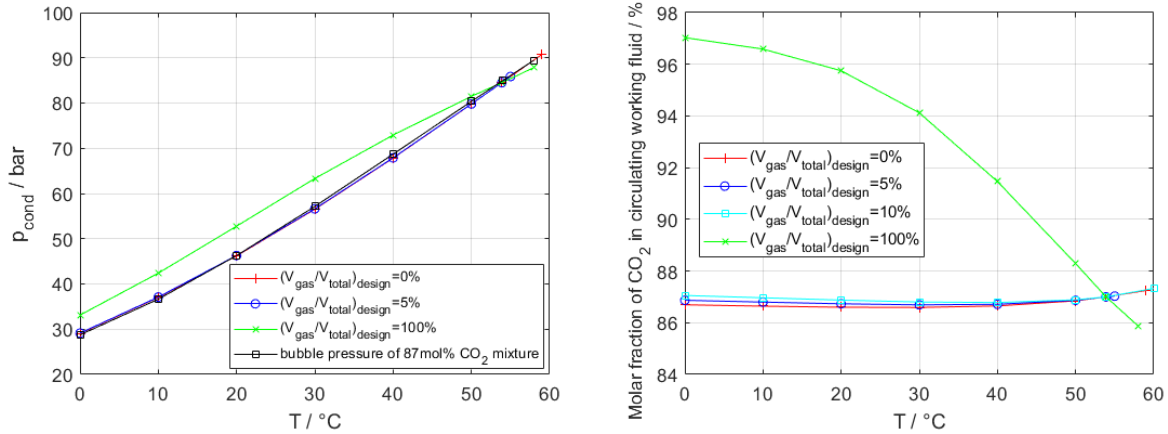


Figure 8. Results of VLE calculations, left: condensation pressure, right: circulating flow composition as a function of condensation temperature.

3.2 Turbine efficiency

For turbine design A, the condensation pressure variation results in lower pressure ratio relative to the design point at the minimum operating condensation temperature, as shown in Figure 9. The efficiency in this case drops from around 93% to about 84% as a result of decreasing the pressure ratio by increasing the condensation temperature. It has been found that reducing the pressure ratio by increasing the outlet pressure deteriorates the performance significantly due to the flow separation in the last turbine stages. When the pressure ratio is increased, as for turbine design B, the efficiency nearly remains constant. It can be noted that both designs are operating in a narrow range of mass flow ratios which is the case when the outlet pressure is varied to control the mass flow-rate as reported in Figure 7.

In case of part-load operation, the inlet pressure is varied while maintaining the same inlet temperature and outlet pressure. The same trends are obtained for the relation between the pressure ratio and mass flow rate for both turbine designs at part-load. However, the efficiencies are different because turbine design A is operating at part-load at an outlet pressure higher than the design outlet pressure although turbine A's design efficiency is 3 percentage points higher than design efficiency of B. It can be seen that turbine design B can operate over a wider range of mass flow-rate because this case-study is performed at the normal condensation temperature compared to case study A which is done at a point different from the operating point.

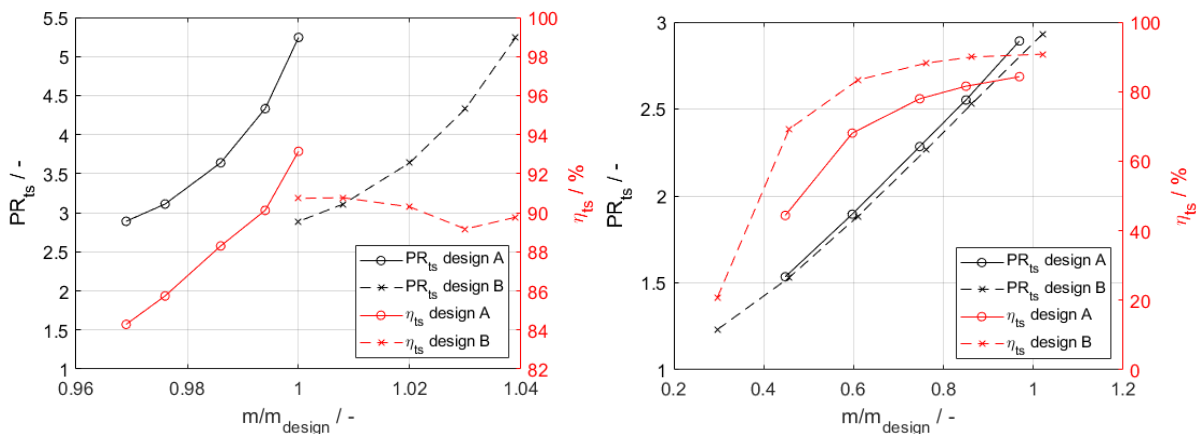


Figure 9. Off-design behavior of turbine, left: sliding condensation pressure, right: part-load.

3.3 Cycle efficiency: influence of turbine design and ambient temperature

Both cycles with the two turbine designs show higher efficiencies at lower condensation temperatures, see Figure 10. When comparing the design cycle efficiency, cycle A (designed for lowest condensation temperature) shows a higher efficiency than cycle B (design for highest temperature). Nonetheless, the cycle B curve lies at higher efficiencies for all specific temperatures.

The trends in heat input and rejection suggest the design cases for the primary heat exchanger and ACC: these differ from the design case of the turbine and working fluid, because lowest condensation temperatures require highest heat input. Exploiting the higher cycle efficiency under these conditions also benefits the hybrid PV-CSP concept as it leads to a higher electricity output during the night, when there are lower ambient temperatures.

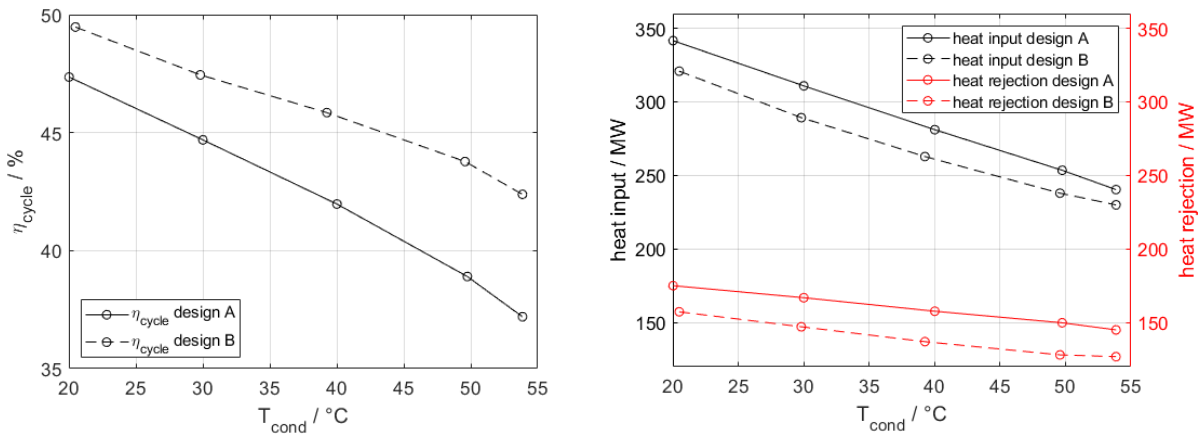


Figure 10. Cycle results for sliding condensation pressure method for turbine designs A, B.

3.4 Cycle efficiency: possible part-load designs

The early drop in efficiency shown in Figure 11 makes cycle A turbine design and operation highly unfavorable. The better choice would be to design for the smallest pressure drop and keep the condensing temperature at the design (highest) level by controlling the fan speed. Then, changing the inlet pressure only results in a moderate loss of efficiency in part-load operation. For 60% mass flow rate in part-load of design B, the heat input can be reduced to 30% of its design value.

The choice of degree of part-load operation depends on what combination of cycle efficiency and reduced heat input can be accepted. This answer can only be given for a specific system including the PV, TES and specific boundary conditions.

Ts-diagrams are shown in Figure 12 for pure CO₂ on the left, cycle A in design conditions in the middle and cycle B in part-load conditions on the right. The higher critical temperature of the mixtures can be noticed. The isobaric lines of mixtures in the two-phase region are sloped, so, condensation happens at a wide temperature glide. Since the recuperator is oversized in part-load conditions, the inlet temperature into the primary heat exchanger is higher than in design conditions. Due to the smaller pressure ratio in part-load, the working fluid does not cool down as much as in design case.

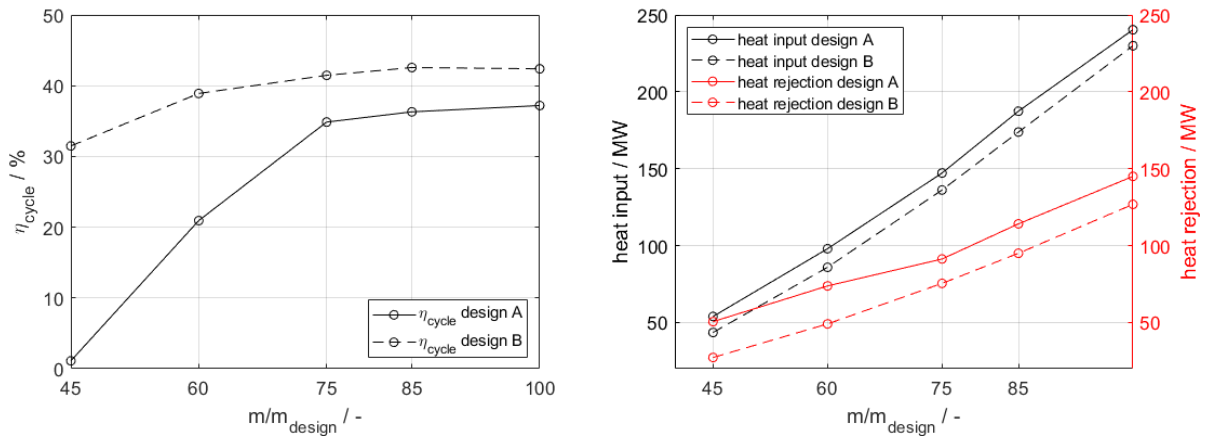


Figure 11. Cycle results for part-load operation for two turbine designs.

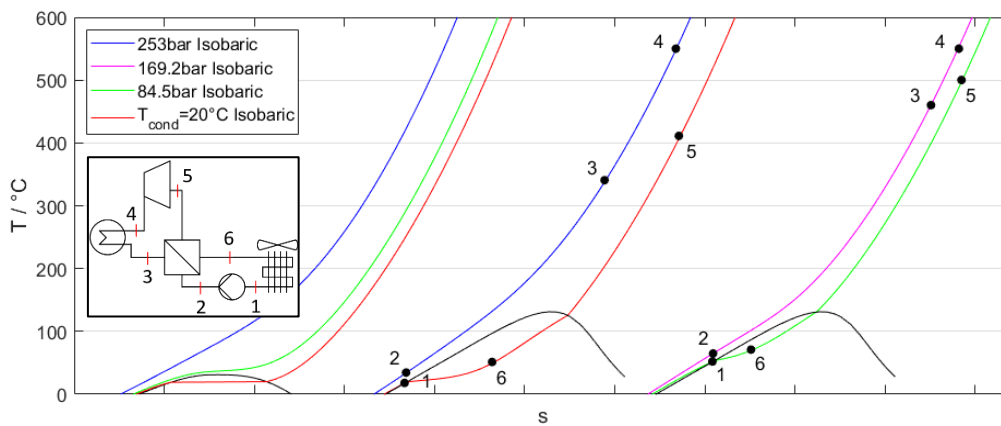


Figure 12. Ts-diagrams for left: pure CO_2 cycle, middle: cycle A in design conditions, right: cycle B in part-load $m/m_{\text{design}} = 60\%$.

3.5 ACC design and correlation of ambient and condensation temperature

The results from the ACC recalculation for cycle A in sliding condensation pressure method are presented in Figure 13. The correlation between air inlet temperature and condensation temperature is nearly linear with a factor of 1.19. This means that as the mass flow slightly reduces with increasing condensation pressure, the pinch between air inlet and working fluid outlet temperature can be reduced. The temperature difference between air inlet and outlet nearly stays the same.

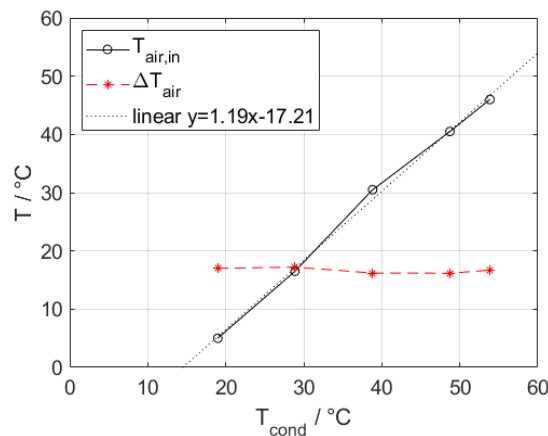


Figure 13. Results from ACC: correlation of ambient air temperature with condensation temperature for sliding condensation pressure method in cycle A.

4. Conclusions and Outlook

This paper has presented off-design operation of a dry-cooled recuperated Rankine cycle operating with a zeotropic mixture of C_6F_6/CO_2 . Off-design conditions on the one hand were part-load conditions with a reduced mass flow rate at high heat sink temperatures. Also, cycle performance was evaluated for the sliding condensation pressure operation, where the condensation temperature of the cycle is allowed to change with a varied heat sink temperature. The impact of two design approaches for the turbine was investigated by a case study. Turbine A and turbine B were designed for the highest and lowest pressure ratio.

The results show that defining the turbine design conditions significantly impacts the thermodynamic performance of the system. Exploiting a lower air temperature for condensation generally results in higher cycle efficiencies. The design efficiency of the cycle with turbine B is higher than of the cycle with turbine A. However, for a specific condensation temperature, cycle A outperforms cycle B by 2.1 to 3.7 percentage points of efficiency. The performance of cycle A seems to be too weak for relevant part-load operation conditions. The turbine A efficiencies are much lower than turbine B's because both inlet and outlet pressure are far from their design values. If choosing system B, the primary heat exchanger, condenser and TES would need to be designed for a different design case than the turbine, namely for the lowest condensation temperature.

For a concrete system with a defined location, the design point for the components must be chosen carefully to find the optimum between bigger sized components for conditions that only occur sparsely during the year and smaller components and a slightly deteriorated cycle performance. The higher investment cost for cycle components may be justified as increasing the power cycle's performance means reducing the solar field size for the same power output and saving investment cost there.

Future work will improve the models used in this analysis, take a correlation between ambient air temperature and available heat input into account and study the impact on the particle-to- sCO_2 heat exchanger and the TES. Also, design B will be compared to the competing operation to sliding condensation pressure: saving electricity with variable fan speed and, thus, keeping the condensation temperature at the highest (the design) value which would then have no impact on cycle performance.

Data availability statement

The data is available at <https://doi.org/10.5281/zenodo.8006758>.

Author contributions

Viktoria Illyés: Conceptualization; Methodology, Formal analysis, Writing – Original Draft; Salma Salah: Software – turbine design, Writing – Original Draft; Writing – Review & Editing; Abdelrahman Abdeldayem: Software – turbine 3D modelling and CFD- turbine off-design and part-load analysis; Writing – Review & Editing; Andreas Werner: Supervision, Writing - Review & Editing; Abdunaser Sayma: Funding acquisition; Giampaolo Manzolini: Project administration; Funding acquisition; Markus Haider: Writing – Review & Editing; Funding acquisition

Competing interests

The authors declare no competing interests.

Funding

The SCARABEUS project has received funding from European Union's Horizon 2020 research program under grant agreement N°814985.

Acknowledgement

The authors thank Ettore Morosini for providing results for part 4 condenser calculation.

References

1. Xing Ju, Chao Xu, Yangqing Hu, Xue Han, Gaosheng Wei, Xiaoze Du, "A review on the development of photovoltaic/concentrated solar power (PV-CSP) hybrid systems", *Solar Energy Materials and Solar Cells*, Volume 161, Pages 305-327, Mar. 2017, <https://doi.org/10.1016/j.solmat.2016.12.004>.
2. Alberto Boretti, "Cost and production of solar thermal and solar photovoltaics power plants in the United States", *Renewable Energy Focus*, Volume 26, Pages 93-99, Sep. 2018, <https://doi.org/10.1016/j.ref.2018.07.002>.
3. Daniel S. Codd, Antoni Gil, Muhammad Taha Manzoor, Melanie Tetreault-Friend, "Concentrating Solar Power (CSP)—Thermal Energy Storage (TES) Advanced Concept Development and Demonstrations". *Curr Sustainable Renewable Energy Rep* 7, 17–27, Apr. 2020, <https://doi.org/10.1007/s40518-020-00146-4>.
4. Francesco Crespi, Pablo Rodríguez de Arriba, David Sánchez, Antonio Muñoz, "Preliminary investigation on the adoption of CO₂-SO₂ working mixtures in a transcritical Recompression cycle", *Applied Thermal Engineering*, Volume 211, 118384, Jul. 2022, <https://doi.org/10.1016/j.applthermaleng.2022.118384>.
5. Anish Modi, Fredrik Haglind, A review of recent research on the use of zeotropic mixtures in power generation systems, *Energy Conversion and Management*, Volume 138, Pages 603-626, Apr. 2017, <https://doi.org/10.1016/j.enconman.2017.02.032>.
6. G. Di Marcoberardino, E. Morosini, D. Di Bona, P. Chiesa, C. Invernizzi, P. Iora, G. Manzolini, "Experimental characterisation of CO₂ + C₆F₆ mixture: Thermal stability and vapour liquid equilibrium test for its application in transcritical power cycle", *Applied Thermal Engineering*, Volume 212, Jul. 2022, <https://doi.org/10.1016/j.applthermaleng.2022.118520>.
7. Li Zhao, Junjiang Bao, The influence of composition shift on organic Rankine cycle (ORC) with zeotropic mixtures, *Energy Conversion and Management*, Volume 83, Pages 203-211, Jul. 2014, <https://doi.org/10.1016/j.enconman.2014.03.072>.
8. Enhua Wang, Zhibin Yu, Fujun Zhang, Investigation on efficiency improvement of a Kalina cycle by sliding condensation pressure method, *Energy Conversion and Management*, Volume 151, Pages 123-135, Nov. 2017, <https://doi.org/10.1016/j.enconman.2017.08.078>.
9. Giampaolo Manzolini, Marco Binotti, Ettore Morosini, David Sanchez, Francesco Crespi, Gioele Di Marcoberardino, Paolo Iora and Costante Invernizzi, "Adoption of CO₂ blended with C₆F₆ as working fluid in CSP plants", *AIP Conference Proceedings* 2445, 090005 (2022); <https://doi.org/10.1063/5.0086520>.
10. S. I. Salah, F. Crespi, M. T. White, A. M. Noz, A. Paggini, M. Ruggiero, D. Sánchez, A. Sayma, "Axial turbine flow path design for concentrated solar power plants operating with CO₂ mixtures", *Appl. Thermal Eng.*, Volume 230, Part A, Jul. 2023, <https://doi.org/10.1016/j.applthermaleng.2023.1206124>.
11. R. H. Aungier, "Turbine Aerodynamics: Axial Flow and Radial-Inflow Turbine Design and Analysis". ASME PRESS, 2006, <https://doi.org/10.1115/1.802418>.

12. V. Illyés, E. Morosini, M. Doninelli, P. David, X. Guerif, A. Werner, G. Di Marcoberardino, G. Manzolini, "Design of an air-cooled condenser for CO₂-based mixtures: model development, validation and heat exchange gain with internal Microfins", Proceedings of ASME Turbo Expo, Oct. 2022, <http://dx.doi.org/10.1115/GT2022-82438>.
13. A. Cavallini, D. Del Col, L. Doretti, M. Matkovic, L. Rossetto, C. Zilio and G. Censi, Condensation in Horizontal Smooth Tubes: A New Heat Transfer Model for Heat Exchanger Design, *Heat Transfer Engineering*, pp. 31-38, 2006.
14. K. J. Bell and M. A. Ghaly, An Approximate Generalized Design Method for Multicomponent/Partial Condenser, *AIChESymp. Ser.*, vol. 69, pp. 72-79, 1973.
15. D. Del Col, A. Bisetto, M. Bortolato, D. Torresin and L. Rossetto, Experiments and updated model for two phase frictional pressure drop inside minichannels, *International Journal of Heat and Mass Transfer*, pp. 326- 337, Dec. 2013, <https://doi.org/10.1016/j.ijheatmasstransfer.2013.07.093>.
16. H. Navarro and L. Cabezas-Gómez, Effectiveness-ntu computation with a mathematical model for cross-flow heat exchangers, *Brazilian Journal of Chemical Engineering*, p. 509–521, Oct. 2007.